

BBAMEM 74687

# Time-resolved fluorescence anisotropy studies on the interaction of biologically active polycations with phospholipid membranes

Tomiki Ikeda, Bong Lee, Hideki Yamaguchi and Shigeo Tazuke

Photochemical Process Division, Research Laboratory of Resources Utilization, Tokyo Institute of Technology, Nagatsuta, Midori-ku, Yokohama (Japan)

(Received 6 June 1989)

Key words: Fluorescence anisotropy; Polycationic biocide; Phospholipid membrane; Polycation–membrane interaction

Interaction of a polymeric in-chain quaternary ammonium salt with phospholipid bilayer membranes was studied by time-resolved fluorescence spectroscopy with the aid of a picosecond time-correlated single photon counting system (instrument response function, 70 ps FWHM). Particular attention was paid to a phenomenon of polycation-induced fluidization of the membranes, which was well evaluated by time-resolved fluorescence anisotropy measurements. The fluorescence anisotropy,  $r(t)$ , of 1,6-diphenyl-1,3,5-hexatriene (DPH) embedded in the membranes was analyzed based on the wobbling-in-cone model. Strong interaction was observed between the polycation and a negatively charged phosphatidic acid membrane as demonstrated by a large decrease of residual polarization value on adding the polycation to the acidic phospholipid dispersion. This means that the cone angle of the wobbling-in-cone motion of the DPH molecule increases by the addition of the polycation, indicative of the polycation-induced fluidization of the acidic membrane. On the other hand,  $r(t)$  of DPH embedded in a zwitterionic phosphatidylcholine membrane was not affected significantly by the addition of the polycation, which is presumably due to non-binding of the polycation to the zwitterionic membrane. Our results clearly indicate that the polycationic disinfectant interacts strongly with negatively charged membranes, inducing fluidization of the membranes.

## Introduction

Cationic disinfectants are major antibacterial agents widely used at present time, which include biguanides and quaternary ammonium salts [1]. Although they are mainly in the form of a monomer (e.g., cetrimide and benzalkonium chloride) and a dimer (e.g., chlorhexidine) [1], many studies on the antibacterial activity of polymeric forms of the cationic disinfectants have been reported because of their promising advantages over the monomeric or dimeric forms of the disinfectants [2]. The first successful example of the polycationic forms of antibacterial agents appeared as early as in the 1950's when Katchalsky et al. found that basic polypeptides such as polylysine, polyornithine and polyarginine ex-

hibited high antibacterial activities against such species as *Escherichia coli* and *Staphylococcus aureus*, while their monomeric amino acids were inactive [3,4].

Apart from polypeptides, Rembaum [5] disclosed antibacterial activity of polyionenes, in-chain quaternary ammonium salts with polymeric forms. They reported that while quaternary ammonium salts with monomeric forms were inactive, their polymeric forms exhibited high antibacterial activity against *E. coli* and *S. aureus*. Poly(hexamethylenebiguanide hydrochloride) (PHMB), a polymeric in-chain biguanide, was found to possess higher activity than those of monomeric and dimeric forms of biguanide compounds, and is in fact one of few examples of polymeric drugs practically in use [6,7].

Other examples of polycations with antibacterial activity include polyacrylates and polymethacrylates with side-chain biguanide moieties, and vinyl polymers with side-chain quaternary ammonium salts [8,9]. Antibacterial assessment of these polycations revealed that these polycations exhibited much higher activity against both Gram-positive and Gram-negative species than the corresponding low molecular weight analogues [8]. Furthermore, with the aid of well-characterized samples with various molecular weights and narrow molecular

Abbreviations: DPH, 1,6-diphenyl-1,3,5-hexatriene; DPPC, dipalmitoyl-L- $\alpha$ -phosphatidylcholine; DPPA, dipalmitoyl-L- $\alpha$ -phosphatidic acid; FWHM, full width at half maximum;  $T_m$ , gel-to-liquid crystalline phase transition temperature.

Correspondence: Tomiki Ikeda, Photochemical Process Division, Research Laboratory of Resources Utilization, Tokyo Institute of Technology, 4259, Nagatsuta, Midori-ku, Yokohama 227, Japan.

weight distributions, we found that the antibacterial activity of these polycations was strongly dependent on molecular weight and an optimum molecular weight region was present for the antibacterial activity [9].

The mode of action of the polycationic disinfectants has been extensively studied and the following sequence of elementary processes has been proposed [7,9]: (1) adsorption onto the bacterial cell surfaces; (2) diffusion through cell walls; (3) absorption onto the bacterial cytoplasmic membranes; (4) disorganization of the membrane structure; (5) leakage of  $K^+$  ions and the other cytoplasmic constituents; (6) death of the cells. Although cytological studies revealed that the crucial process in the lethal action of the polycations is their interaction with the cytoplasmic membranes [9], it is still obscure how the polycations interact with the membranes.

There are two possible sites in the cytoplasmic membranes of the bacterial cells with which the polycations interact. They are membrane proteins and phospholipids. Physiological studies on the mode of action of PHMB have shown that this polycation disrupts the membrane physically and the polycation-membrane interaction is nonspecific [7]. This observation suggests interaction of the polycation with matrix phospholipids [7]. Furthermore, studies on small molecular weight cationic disinfectants have revealed that the site of their interaction is phospholipids of the microbial membranes [10].

In this paper, we explored the interaction of polycation with phospholipid bilayer membranes as a model system for the polycation/bacterial cytoplasmic membrane interactions by time-resolved fluorescence spectroscopy with the aid of a picosecond time-correlated single photon counting system. Particular attention was paid to a phenomenon of polycation-induced fluidization of the membrane, which was well evaluated by the time-resolved fluorescence anisotropy measurements. Another point to which we paid special attention was the effect of the polar head group of the phospholipid on the polycation-membrane interaction, since it is well known that the bacterial cytoplasmic membranes are composed of zwitterionic and acidic phospholipids [11]. In this study, we used two kinds of the phospholipids: one is a zwitterionic phosphatidylcholine and the other is an acidic phosphatidic acid which is negatively charged at physiological pH.

## Materials and Methods

**Materials.** The structures of the organic cations used in this study and their abbreviations are shown in Fig. 1.

**Dimethyldibenzylammonium bromide (1).** *N,N*-Dimethylbenzylamine (3.5 g, 26 mmol) and benzyl bromide (4.4 g, 26 mmol) were reacted in methanol (100 ml) for

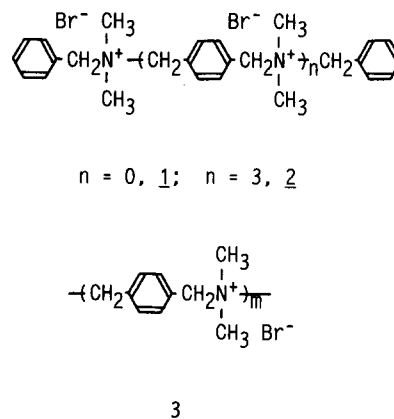


Fig. 1. Structure of organic cations used in this study.

15 h at room temperature. After removing the solvent, the crude product was recrystallized twice from an acetone/2-propanol mixture. Yield, 4.1 g (52%);  $^1\text{H-NMR}$  ( $\text{CD}_3\text{OD}$ ),  $\delta$ : 3.0 (6H, s), 4.8 (4H, s), 7.6 (10H, m).

***N,N,N',N'*-Tetramethyl-*p*-xylylenediamine.** This compound was prepared by the procedure described in the literature [12] with modification.  $\alpha,\alpha'$ -Diamino-*p*-xylene (24 g, 0.18 mol) and formalin (37% formaldehyde in aqueous solution) were added to 94 g of formic acid (85%). The reaction mixture was stirred at room temperature for 1 h and then refluxed for 2.5 h. After cooling, 20 ml of hydrochloric acid (35%) was added. After the solvent was removed, the remaining white solid was dissolved in water and the solution was made alkaline with sodium hydroxide solution. The product was extracted with ether and distilled under reduced pressure (121–122°C/11 mmHg). Yield, 21 g (61%);  $^1\text{H-NMR}$  ( $\text{CDCl}_3$ ),  $\delta$ : 2.2 (12H, s), 3.43 (4H, s), 7.32 (4H, s).

**Dimethylbenzyl-(*p*-*N,N*-dimethylaminomethyl)benzylammonium bromide.** *N,N,N',N'*-Tetramethyl-*p*-xylylenediamine (10 g, 52 mmol) and benzyl bromide (1.1 g, 6.5 mmol) were dissolved in acetone and the mixture was left at room temperature for 10 h. The precipitated diammonium salt formed was removed by filtration. After removing the solvent from the filtrate, ether was added and the product was extracted with ether. The product was finally purified by column chromatography on  $\text{Al}_2\text{O}_3$  (acetone/methanol, 7:3, v/v). Yield, 1.0 g (43%);  $^1\text{H-NMR}$  ( $\text{CD}_3\text{OD}$ ),  $\delta$ : 2.26 (6H, s), 3.04 (6H, s), 3.55 (2H, s), 4.87 (4H, s), 7.3–7.9 (9H, m).

***p*-Xylylenebis[*N,N*-dimethyl-4-(dimethylbenzylammoniomethyl)benzylammonium]tetrabromide (2).** Dimethylbenzyl-(*p*-*N,N*-dimethylaminoethyl)benzylammonium bromide (5.0 g, 14 mmol) and *p*-xylylene dibromide (1.7 g, 6.4 mmol) were dissolved in a mixture of dimethyl sulfoxide/water (20:5, v/v) and left at room temperature for 60 h. The reaction mixture was then poured into a large excess of acetone, and the precipitated product was recovered, dried under vacuum and recryst-

tallized from ethanol/methanol. Yield, 96%;  $^1\text{H-NMR}$  ( $\text{CD}_3\text{OD}/\text{D}_2\text{O}$ ),  $\delta$ : 2.85–3.35 (24H, broad), 4.30–5.00 (16H, broad), 7.40–7.95 (22H, m).

The monomer (1) and the tetramer (2) were finally purified by preparative gel-filtration chromatography on Bio-Gel P2 using ammonium acetate buffer as eluent.

*Poly[(dimethylimino)-p-xylylene bromide] (3).* *p*-Xylylene dibromide (4.0 g, 15 mmol) and *N,N,N',N'*-tetramethyl-*p*-xylylenediamine (2.9 g, 15 mmol) were heated in 50 ml of dimethyl sulfoxide to 70°C. After several minutes, precipitation of the polymer was observed, so that 50 ml of water was added to the reaction mixture so as to keep the reaction mixture homogeneous. After 4 h, the mixture was poured into an excess of acetone and the precipitated polymer was recovered by filtration. Yield, 6.4 g (94%).

The molecular weight of the polycation was measured in phosphate buffer (pH 7.4) with a Chromatix KMX-6 low-angle laser light-scattering photometer as  $4 \cdot 10^4$  (degree of polymerization, 170).

*Other materials.* Dipalmitoyl-L- $\alpha$ -phosphatidylcholine (DPPC), dipalmitoyl-L- $\alpha$ -phosphatidic acid (DPPA) were obtained from Sigma and used without further purification. 1,6-Diphenyl-1,3,5-hexatriene (DPH) was obtained from Aldrich and recrystallized from acetone.

*Fluorescence measurements.* Steady-state fluorescence measurements were performed with a Hitachi F-4000 fluorescence spectrometer.

Fluorescence lifetimes and fluorescence anisotropy decays were measured with a picosecond time-correlated single photon counting apparatus [13]. A synchronously pumped, cavity-dumped dye laser (Spectra Physics 375B and 344S) operated with a mode-locked Nd:YAG laser (Spectra Physics 3460 and 3240) was the excitation pulse source with a pulse width of 6 ps (FWHM). We obtained a frequency-doubled pulse for the excitation of the samples through a KDP crystal (Inrad 531). Fluorescence from the samples was detected at right angles to the excitation pulse through a monochromator (JASCO CT-25C) with a microchannel-plate photomultiplier (Hamamatsu R1564U-01). Signals from the photomultiplier were amplified (HP 8447P), discriminated (Ortec 583) and used as a stop pulse for a time-to-amplitude converter (TAC; Ortec 457). A start pulse was provided from a fast photodiode (Antel AR-S2) monitoring a laser pulse through a discriminator (Ortec 436). Data were stored in a multichannel analyzer (Canberra 35 Plus) and then transferred to a microcomputer (NEC 9801) where decay analysis was performed by an iterative non-linear least-squares method. The instrument response function of the whole system was 70 ps FWHM. For fluorescence anisotropy measurements, a vertically polarized light pulse was obtained through a Babinet-Soleil compensator, and  $I_{\parallel}(t)$  and  $I_{\perp}(t)$  were measured alternatively through a polarizer which was rotated periodically in order to eliminate any

artifacts due to long-term laser instability. Here,  $I_{\parallel}(t)$  and  $I_{\perp}(t)$  represent the fluorescence intensities observed with parallel and perpendicular orientation of the polarizer placed in the monitor side to the vertically polarized excitation pulse, respectively. A depolarizer was also placed just before the monochromator to remove anisotropic characteristics of the monochromator against  $I_{\parallel}(t)$  and  $I_{\perp}(t)$ .

Liposome solutions for the fluorescence measurements were prepared by dispersing lipids in 50 mM phosphate buffer (pH 7.4), followed by sonication. Phospholipid was dissolved in chloroform, and to this solution DPH dissolved in tetrahydrofuran was added. The solvent was then removed under  $\text{N}_2$ , followed by storage under high vacuum. To the dried lipid film containing DPH was added 10 ml of the phosphate buffer and then sonication was performed above the phase transition temperature ( $T_m$ ) of the lipid with a Tomy UR-200 probe-type ultrasonic disruptor. Final concentrations of the lipids and DPH were 1 mM and 1.5  $\mu\text{M}$ , respectively. For measurements of fluorescence of DPH in the presence of the organic cations, a small portion (up to 40  $\mu\text{l}$ ) of the concentrate of the organic cations in the same phosphate buffer was added by means of a microsyringe to a 4-ml portion of the liposome solution, and the resulting solution was mixed vigorously. Concentrations of the organic cations were expressed in  $\mu\text{M}$  on the basis of the positively charged N atoms. All measurements were conducted in a quartz cell under argon atmosphere.

*Analysis.* Fluorescence anisotropy at time  $t$ ,  $r(t)$ , is defined by

$$r(t) = \frac{I_{\parallel}(t) - I_{\perp}(t)}{I_{\parallel}(t) + 2I_{\perp}(t)} = \frac{I_D(t)}{I_T(t)} \quad (1)$$

where  $I_T(t)$  and  $I_D(t)$  represent the total fluorescence intensity and the difference of intensity between vertical and horizontal components at time  $t$ , respectively.

Decay of anisotropy for a DPH molecule in phospholipid bilayers can be separated into two components: one is a rapid decaying component at the initial stage and the other is a constant component [14]. The decay curve can, thus, be expressed as

$$r(t) = (r_0 - r_{\infty}) \exp(-t/\phi) + r_{\infty} \quad (2)$$

where  $r_0$  and  $r_{\infty}$  represent the fluorescence anisotropy at  $t = 0$  and at  $t = \infty$ , respectively, and  $\phi$  is the relaxation time for rotational diffusion of DPH molecule [14].

In order to obtain the best fit curves based on Eqn. 2, the decay curves of  $I_T(t)$  were analyzed first by the weighted linear least-squares method and the least-squares fits for the curves of  $I_D(t)$  were performed according to the modified equation,  $r(t) \cdot I_T(t)$ , which contains a decaying component and a growing component due to lamp excitation [13].

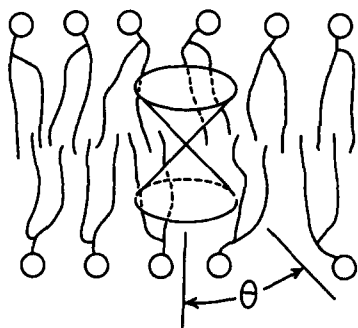


Fig. 2. Schematic illustration of the wobbling-in-cone model.

Free volume around the DPH molecule was estimated as cone angle ( $\theta$ ) according to the wobbling-in-cone model (Fig. 2), in which the long axis of the rod-shaped DPH molecule was assumed to wobble uniformly in a cone of semiangle  $\theta$  [14]. This model suggests that  $\theta$  can be calculated by

$$r_{\infty}/r_0 = [(1/2) \cos \theta (1 + \cos \theta)]^2 \quad (3)$$

## Results

### Steady-state fluorescence anisotropy

Temperature dependence of the steady-state fluorescence anisotropy,  $r_s$ , for DPH embedded in the DPPC and DPPA membranes in the absence and presence of the polycation 3 is shown in Fig. 3. Abrupt changes of  $r_s$  observed in the absence of the polycation at approx. 40°C for the DPPC membrane and at approx. 60°C for the DPPA membrane are due to the phase transition of the phospholipid membranes. In the case of the zwitterionic DPPC membrane, no significant effect of the polycation on  $r_s$  was observed over the whole temperature range below and above  $T_m$  as shown in fig. 3A, while the polycation brought about significant decrease of  $r_s$  in the acidic DPPA membrane (Fig. 3B). With increasing concentration of 3,  $r_s$  was found to decrease and at [3] = 50  $\mu$ M,  $r_s$  at 56°C was less than half of the

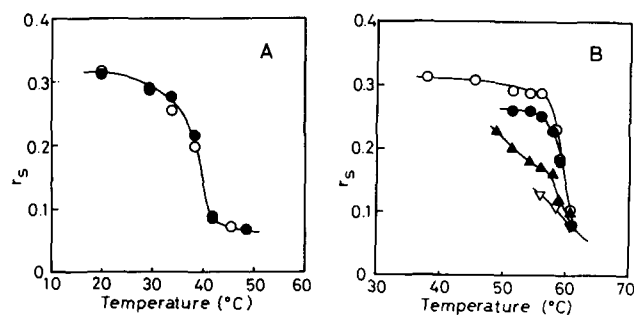


Fig. 3. Temperature dependence of steady-state fluorescence anisotropy,  $r_s$ , of DPH embedded in DPPC(A) and DPPA(B) membranes. (A)  $\circ$ , in the absence of the polycation 3;  $\bullet$ , in the presence of the polycation 3 (50  $\mu$ M). (B) Concentration of 3: ( $\circ$ ), 0; ( $\bullet$ ), 6.3  $\mu$ M; ( $\blacktriangle$ ), 12.5  $\mu$ M; ( $\nabla$ ), 50  $\mu$ M.

value observed in the absence of the polycation. Unfortunately, in the case of the DPPA membrane, precipitation was observed at low temperatures in the presence of high concentration of the polycation, thus measurements were performed from higher temperature and the results obtained for the cooling process are shown in Fig. 3B. Note that fluidization effect of the polycation on the acidic DPPA membrane in the gel phase was observed even at the concentration eight times lower than that of the DPPC membrane (6.3  $\mu$ M). Furthermore, clear transition was not observed at higher concentrations of the polycation. These results clearly indicate that electrostatic attraction undoubtedly plays an important role in the polycation-membrane interaction.

### Lifetime measurements of DPH embedded in the membranes

Results of the fluorescence decay analyses of DPH embedded in the DPPC and DPPA membranes have shown that in all cases examined, in the DPPC and DPPA membranes, in the absence and presence of the polycation and over the whole temperature range studied, the fluorescence decays were satisfactorily analyzed by the double-exponential function in the form of

$$A_1 \exp(-t/\tau_1) + A_2 \exp(-t/\tau_2)$$

with lifetimes of  $\tau_1 \approx 10$  ns and  $\tau_2 \approx 2$  ns as judged by reduced chi-square ( $\chi^2$ ) and Durbin-Watson (DW) parameters ( $0.9 < \chi^2 < 1.1$ ;  $1.85 < DW$ ). The short lifetime components are minor and their contribution to the total fluorescence intensity is only several percent as judged by the parameter,  $\alpha_2 (= A_2\tau_2/\sum A_i\tau_i) \leq 0.06$ .

Temperature dependence of the lifetimes of DPH in the membranes is clearly visualized in Fig. 4 where the lifetimes of the long and short components are plotted as a function of temperature. In Fig. 4 are also included the lifetimes in the presence of the polycation 3. It is recognized that the lifetimes are not significantly affected by the polycation both in the DPPC and DPPA

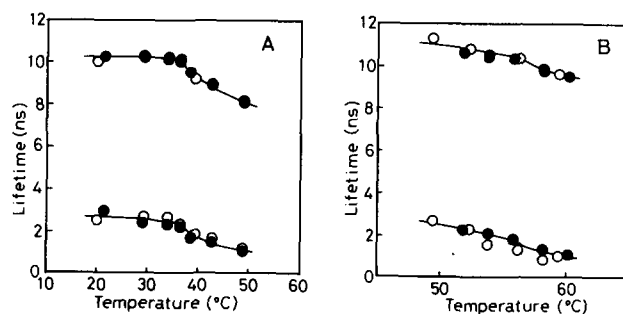


Fig. 4. Temperature dependence of lifetimes of DPH embedded in DPPC (A) and DPPA (B) membranes.  $\circ$ , in the absence of polycation 3;  $\bullet$ , in the presence of polycation 3. [3] is 50  $\mu$ M for the DPPC membrane and 12.5  $\mu$ M for the DPPA membrane.

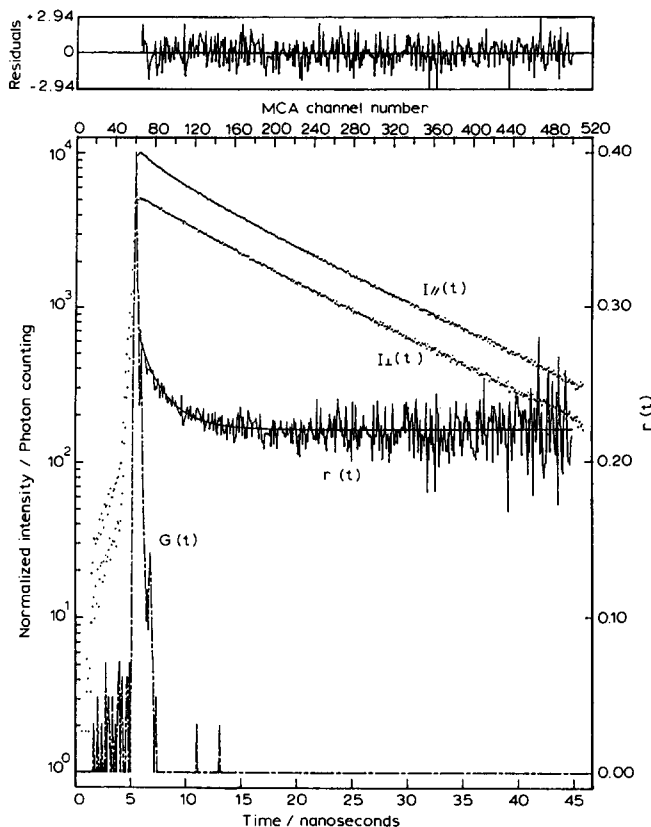


Fig. 5. Polarized fluorescence decays,  $I_{||}$  and  $I_{\perp}$ , instrument response function,  $G(t)$ , and anisotropy decay,  $r(t)$ , of DPH embedded in DPPC membrane.  $\lambda_{ex} = 318$  nm,  $\lambda_{em} = 450$  nm.

membranes below and above  $T_m$  of the lipid membranes.

#### Time-resolved fluorescence anisotropy

An example of fluorescence anisotropy decay profiles is shown in Fig. 5 where  $I_{||}(t)$ ,  $I_{\perp}(t)$  and  $r(t)$  of DPH embedded in the DPPC membrane are shown as a function of time. In Fig. 5 is also shown the best-fit curve based on Eqn. 2 and on top the residuals for the fit. Although the total fluorescence decays had two components as described above, no significant improvement in goodness of the fitting was observed when  $r(t)$  was analyzed by double exponential function in the form of

$$r(t) = (r_0 - r_{\infty})[K \exp(-t/\phi_1) + (1 - K) \exp(-t/\phi_2)] + r_{\infty} \quad (4)$$

where  $K$  is a constant. This means that the single exponential decay law as expressed by Eqn. 2 is satisfactory enough to describe the anisotropy decay behavior of DPH embedded in the DPPC and DPPA membranes. The relaxation times for the rotational diffusion of DPH ( $\phi$ ) in the membranes determined by the fitting procedure of the observed  $r(t)$  based on Eqn. 2 are plotted in fig. 6 as a function of temperature. In the case of DPH embedded in the DPPC membrane,  $\phi$  was

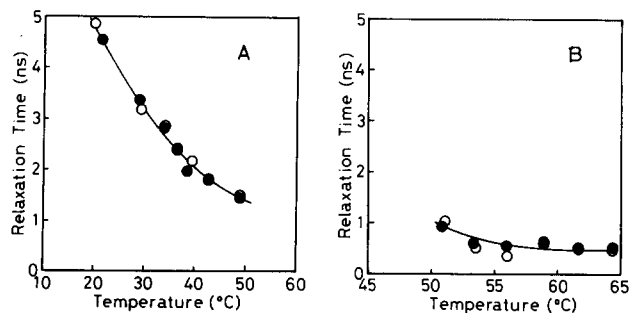


Fig. 6. Temperature dependence of the relaxation times for the rotational diffusion of DPH in DPPC (A) and DPPA (B) membranes.  $\circ$ , in the absence of polycation 3;  $\bullet$ , in the presence of polycation 3. [3] is  $50 \mu\text{M}$  for the DPPC membrane and  $12.5 \mu\text{M}$  for the DPPA membrane.

found to decrease somewhat monotonically with temperature regardless of the presence of the polycation (Fig. 7A). The  $\phi$  value of DPH incorporated in the DPPA bilayer was also found to decrease with temperature and no drastic change in  $\phi$  was observed at  $T_m$  (Fig. 6B). Furthermore, no significant effect of the polycation on  $\phi$  was observed in both membranes.

Temperature dependence of  $r_{\infty}$  of DPH embedded in the DPPC and DPPC membranes is shown in Fig. 7. The temperature profiles of the  $r_{\infty}$  values are similar between the DPPC and DPPA membranes: the  $r_{\infty}$  values in the gel state are approx. 0.28 and those in the liquid crystalline state are approx. 0.05. This suggests that regardless of the structure of the polar head group both DPPC and DPPA form bilayers with a similar inner structure. As is seen in Fig. 7A, no significant effect of the polycation on  $r_{\infty}$  was observed over the whole temperature range below and above  $T_m$  in the case of DPH embedded in the DPPC membrane. On the other hand, remarkable effect of the polycation on  $r_{\infty}$  was seen in the DPPA membrane as shown in Fig. 7B. The  $r_{\infty}$  values in the presence of  $12.5 \mu\text{M}$  of the polycation were much smaller than those of the pure DPPA membrane particularly in the gel phase.

Physical meanings of these results can be more clearly interpreted in terms of the cone angle ( $\theta$ ) of the wob-

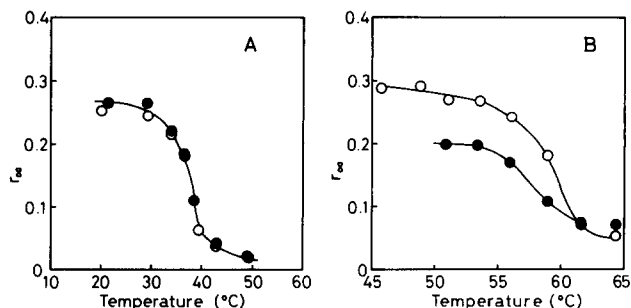


Fig. 7. Temperature dependence of  $r_{\infty}$  of DPH embedded in DPPC (A) and DPPA (B) membranes.  $\circ$ , in the absence of polycation 3;  $\bullet$ , in the presence of polycation 3. [3] is  $50 \mu\text{M}$  for the DPPC membrane and  $12.5 \mu\text{M}$  for the DPPA membrane.

bling-in-cone motion of the DPH molecule. As described in Materials and Methods, the cone angle can be evaluated by Eqn. 3 with  $r_0 = 0.395$ . The values of the cone angle ( $\theta$ ) thus estimated are shown in Fig. 8 as a function of temperature. In the absence of the polycation, the values of  $\theta$  in the gel phase are similar in the DPH/DPPC ( $\approx 39^\circ$ ) and the DPH/DPPA ( $\approx 36^\circ$ ) systems and they increase abruptly at  $T_m$  ( $\approx 40^\circ\text{C}$  for DPPC and  $\approx 60^\circ\text{C}$  for DPPA). This manifests the increase of free volume around the DPH molecules in the membranes associated with the gel-to-liquid crystalline phase transition of the membranes. In the gel state, the membrane is rigid, providing only a small free volume for the DPH molecule to wobble, whereas in the liquid-crystalline state the membrane is fluid enough for the probe molecule to take the wobbling-in-cone motion with a large cone angle. No significant change in  $\theta$  was observed when the polycation 3 was added to the DPH/DPPC system (Fig. 8A). On the other hand, when the polycation was added to the DPH/DPPA system, the  $\theta$  values increased by approx.  $10^\circ$  in the gel phase as seen in Fig. 8B. This result indicates that the polycation induces fluidization of the negatively charged DPPA membrane.

#### Effect of molecular weight

Effect of molecular weight on the mode of interaction of organic cations with phospholipid membranes was explored with the aid of the well-characterized samples of the monomer (1), the tetramer (2) and the polymer (3). Antibacterial assessment of these homologues has shown that both bacteriostatic and bactericidal activities against *Staphylococcus aureus* and *Escherichia coli* increase in the order of  $1 \ll 2 < 3$ . This is exactly the order of increasing molecular weight (Ikeda et al., unpublished results). As in the case of the polycation 3, the lifetimes,  $\phi$  and  $r_\infty$  of DPH embedded in the zwitterionic DPPC membrane were not affected by the monomer and the tetramer. Furthermore, the lifetimes and  $\phi$  values were not influenced significantly

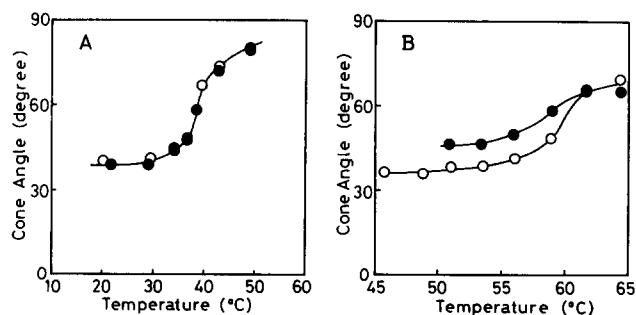


Fig. 8. Temperature dependence of the cone angle ( $\theta$ ) of the wobbling-in-cone motion of DPH embedded in DPPC (A) and DPPA (B) membranes.  $\circ$ , in the absence of polycation 3;  $\bullet$ , in the presence of polycation 3. [3] is  $50\ \mu\text{M}$  for the DPPC membrane and  $12.5\ \mu\text{M}$  for the DPPA membrane.

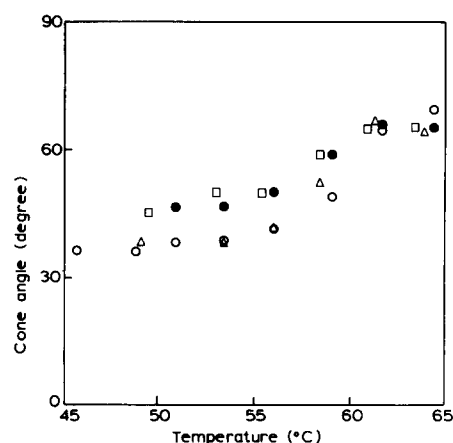


Fig. 9. Cone angles ( $\theta$ ) of the wobbling-in-cone motion of DPH embedded in the DPPA membrane in the presence of various MW quaternary ammonium salts. ( $\circ$ ), in the absence of the cations. In the presence of: ( $\Delta$ ), the monomer 1; ( $\square$ ), the tetramer 2; ( $\bullet$ ), the polymer 3. The concentration of the cations was  $12.5\ \mu\text{M}$  based on the  $\text{N}^+$  units.

by 1 and 2 over the whole temperature range. Only observable that exhibited a clear molecular weight dependence was  $r_\infty$  (so  $\theta$ ) for the DPPA membrane. As shown in fig. 9, the  $\theta$  values in the presence of 1 were similar to those of the pure DPPA membrane. However, the  $\theta$  values in the presence of the tetramer were clearly different from those of the pure DPPA membrane and 1/DPPA system, being rather close to those of 3/DPPA system. These results indicate that while the monomer has no effect, an oligomer with the degree of polymerization (DP) as small as 4 exhibits a large fluidization effect on the negatively charged DPPA membrane, the degree of which is similar to that of the polycation with DP as large as 170.

#### Discussion

Fluorescence anisotropy of DPH has been frequently used for investigation of bilayer membrane fluidity [15]. Since DPH is a polyene hydrocarbon with a stable all-*trans* configuration, the molecule lies along the long acyl chain of phospholipids in the membrane [14]. The transition moments of absorption and fluorescence lie nearly parallel to the long axis of DPH [16]. Under experimental condition used in the present study ( $[\text{DPH}]/[\text{lipid}] = 1/700$ ), contribution of energy migration to fluorescence depolarization is negligible [17]. Furthermore, microaggregated DPH molecules in water, if any, are not fluorescent [16], so that fluorescence anisotropy of DPH only reflects rotational diffusion of the DPH molecules embedded in the hydrocarbon region of the bilayer membranes. Decrease in the fluorescence anisotropy indicates greater freedom for wobbling motion of the probe molecule, in other words, higher fluidity in acyl chain regions [14,16].

The fluorescence decays of DPH in membranes were analyzed by the double-exponential function with lifetimes of approx. 10 ns and approx. 2 ns as shown in Fig. 4. The long-lifetime components had almost constant values of approx. 10 ns below  $T_m$  and their values decreased abruptly around  $T_m$  in both membranes. This tendency is in good agreement with the results reported so far [18,19]. With respect to the nature of the short-lifetime components, it was recently reported that a photodecomposition product of either lipid or DPH is responsible for the 2–3-ns minor-lifetime component often reported for the DPH-containing membranes [18,19]. However, there is some controversy over the origin of the short lifetime component, so that it should be reminded that the exact origin of this component has not been well understood [19]. Whatever is the exact origin of the short lifetime component, the contribution of this component is very small, thus we can safely neglect this component in the analysis.

The primary interaction of the organic cations with DPPA would be to compensate the phosphate charges of DPPA leading to a denser packing of the lipids and a decrease of fluidity. In the present case, however, the polycation induced an increase of the fluidity which presents a more complicated effect. The fluidization induced by the polycation seems to arise from intercalation of the polycation into the membranes. Binding of the polycation to the negatively charged phospholipids may lead to induction of interlipid separation. In this respect, monolayer experiments on the interaction of the polycation with in-chain biguanide groups (PHMB) and the acidic phosphatidylglycerol (PG) were carried out recently. Their results have demonstrated that PHMB expands greatly the monolayer of PG formed at the water/air interface under a constant pressure and increase the monolayer pressure under a constant areas (Eyres and Brown, unpublished results). Electrostatic attraction between the positive charges on the biguanide groups of PHMB and the negative charges of PG is assumed to be the driving force for the complex formation between the polycation and PG molecules. The hydrophobic hexamethylene groups which link the biguanide groups in PHMB are considered to play an important role in expansion of the PG monolayer. They

seem to act as wedges which are inserted into more hydrophobic sites in the membrane, thus producing a larger distance between the PG molecules (Eyres and Brown, unpublished results). In combination with these observations, it seems certain that the polycation 3 as well as the tetramer 2 increase the lateral distance between the DPPA molecules arranged in bilayer in a similar way to that of PHMB and produce more room for the probe molecules to undergo less-hindered motion.

## References

- 1 Franklin, T.J. and Snow, G.A. (1981) in *Biochemistry of Antimicrobial Action*, pp. 58–78, Chapman and Hall, London.
- 2 Gebelein, C.G. and Carraher, C.E. (1982) in *Biological Activities of Polymers* (ACS Symposium Series 186) (Carraher, C.E., Jr. and Genelein, C.G., eds.), pp. 1–9, Washington, DC.
- 3 Katchalsky, E., Bichovski-Slomnitzki, L. and Volcani, B.E. (1952) *Nature* 169, 1095–1096.
- 4 Katchalsky, E. (1964) *Biophys. J.* 4, 9–41.
- 5 Rembaum, A. (1973) *Appl. Polym. Symp.* 22, 299–317.
- 6 Davies, A., Bentley, M. and Field, B.D. (1968) *J. Appl. Bacteriol.* 31, 448–461.
- 7 Broxton, P., Woodcock, P.M. and Gilbert, P. (1983) *J. Appl. Bacteriol.* 54, 345–353.
- 8 Ikeda, T., Yamaguchi, H. and Tazuke, S. (1984) *Antimicrob. Agents Chemother.* 26, 139–144.
- 9 Ikeda, T., Hirayama, H., Yamaguchi, H. and Tazuke, S. (1986) *Antimicrob. Agents Chemother.* 30, 132–136.
- 10 Elferink, J.G.R. and Booij, H.L. (1974) *Biochem. Pharmacol.* 23, 1413–1419.
- 11 Rogers, H.J., Perkins, H.R. and Ward, J.B. (1980) in *Microbial Cell Walls and Membranes*, Chapman and Hall, London.
- 12 Moore, M.L. (1949) in *Organic Reactions Vol. 5* (Adams, R., ed.), p. 323, Wiley, New York.
- 13 Ikeda, T., Lee, B., Kurihara, S., Tazuke, S., Itoh, S. and Yamamoto, M. (1988) *J. Am. Chem. Soc.* 110, 8299–8304.
- 14 Kawato, S., Kinoshita, Jr. K. and Ikegami, A. (1977) *Biochemistry* 16, 2319–2324.
- 15 Bisby, R.H., Cundall R.B., Davenport, L., Johnson, I.D. and Thomas, E.W. (1981) in *Fluorescent Probes* (Beddard, G.S. and West, M.A., eds.), pp. 97–109, Academic, London.
- 16 Shinitzky, M. and Barenholz, Y. (1978) *Biochim. Biophys. Acta* 515, 367–373.
- 17 Davenport, L., Dale, R.E., Bisby, R.H. and Cundall, R.B. (1985) *Biochemistry* 24, 4097–4108.
- 18 Parasassi, T., Conti, F., Glaser, M. and Gratton, E. (1984) *J. Biol. Chem.* 259, 14011–14017.
- 19 Barrow, D.A. and Lentz, B.R. (1985) *Biophys. J.* 48, 221–234.